ARTICLES

Fabrication of Fluorescent Rare Earth Phosphates in Confined Media of Polyelectrolyte Microcapsules

Dmitry G. Shchukin,* Gleb B. Sukhorukov, and Helmuth Möhwald

Max Planck Institute of Colloids and Interfaces, D14424 Potsdam, Germany

Received: May 6, 2004; In Final Form: September 29, 2004

Fluorescent rare earth nanophosphates ($La_{0.95}Eu_{0.05}PO_4$, $Ce_{0.9}Tb_{0.1}PO_4$, and $La_{0.4}Ce_{0.45}Tb_{0.15}PO_4$) were synthesized by reacting the corresponding nitrates exclusively inside PO_4^{3-} loaded poly(styrene sulfonate)/poly(allylamine hydrochloride) polyelectrolyte capsules of 2.4 μm diameter at room temperature. Crystallization conditions inside the polyelectrolyte capsules lead to the fabrication of crystalline nanoparticles with high fluorescence yield without additional thermal treatment. The fluorescence of these nanoparticles is stable at low and neutral pH. The fluorescent rare earth nanophosphates, fabricated inside polyelectrolyte capsules, were characterized by TEM, SEM, and XRD techniques and fluorescence spectroscopy. Resulting nanophosphates are nanorods ca. 15 nm long and 4 nm in diameter, and they are formed near the inner side of the capsule wall.

Introduction

Synthesis of nanostructured composite materials has been of considerable interest for more than two decades. Starting from the 1980s,[1−3] many reliable synthetic procedures were developed, which allow one to obtain in solution a wide range of nanosized materials with determined properties.[4−6] However, most of the nanomaterials, synthesized by a wet method in bulk solution, are amorphous or weakly crystalline and, to achieve high crystallinity of the nanoparticles, additional thermal treatment (annealing) is required. The other possible way to obtain ordered nanomaterial is to create specific crystallization conditions during synthesis (e.g., by reducing the rate of the reaction).

Reactions inside spatially confined micro(nano)volumes could be carried out under conditions impossible for conventional macrovolume: controlled microdiffusion of the reagents, homogeneous distribution of the temperature in microvolumes, and other solvent structure and crystallization conditions.[7,8] As a result, one can obtain both simple nanoparticles in metastable crystal modifications and unique, complex composite nanomaterials. Microemulsions, liposomes, and micelles were successfully applied as examples of the microreactor for fabrication of the crystalline nanoparticles.[9−11]

One of the confined micromedia developed so far is the inner volume of polyelectrolyte capsules. Polyelectrolyte capsules were introduced more than 5 years ago.[12] They are hollow, micron-sized polyelectrolyte spheres formed by electrostatic layer-by-layer assembly[13,14] of oppositely charged polyelectrolytes on the surface of a sacrificial template core ($MnCO_3$, methyl formaldehyde). The polyelectrolyte shell of the capsules possesses regulated permeability, which depends on the pH or ionic strength of the dispersing media.[15] The choice of the sacrificial template particles enables one to produce microcapsules of different size (20 nm to 20 μm) and shape.

Polyelectrolyte capsules were previously demonstrated in several publications[16−20] as suitable microreactors for fabrication of crystalline, nonaggregated nanoparticles[17] or particles in the metastable crystal phase.[18] Here, we examine the possibility of employing polyelectrolyte microcapsules for the synthesis of crystalline, fluorescent rare earth nanophosphates at room temperature. Rare earth phosphates (RE phosphates) are a class of materials with significant technological importance. They are used, for instance, as laser materials, in lightning applications, and as phosphors in cathode ray tubes.[21,22] Nanoparticles of these materials are considered as potentially useful active components in new optoelectronic devices.[23] Recently, a wet synthesis was reported by Haase and co-workers,[24−26] which allows the fabrication of rare earth phosphate nanoparticles with narrow size distribution. Before, the annealing of an oxide−phosphate mixture of rare earths was employed[27−29] to fabricate fluorescent phosphate micropowder. The fluorescence of lanthanide phosphates originates from the transition between d and f electron states of the rare earth (i.e., from their bulk properties of the crystal phase) and does not depend on the size of nanoparticles in contrast to quantum dots.[25,30] Their fluorescence color is adjusted by the rare-earth dopant. Other advantages of RE phosphates are chemical and bleaching stability, high quantum yield, and the possibility of application in biotechnology due to the low toxicity.[31]

The motivation of this work is to explore the possibility of the synthesis of the crystalline RE nanophosphates exclusively inside the capsule microvolume at room temperature. Up-to-date, there are no literature data presenting the fluorescent RE nanophosphates prepared at room temperature. All the methods reported require additional thermal treatment (annealing or

* Author to whom correspondence should be addressed. E-mail: dmitry.shchukin@mpikg-golm.mpg.de. Phone: +49-331-567-9257. Fax: +49-331-567-9202.

10.1021/jp048052o CCC: $27.50
Published on Web 11/16/2004

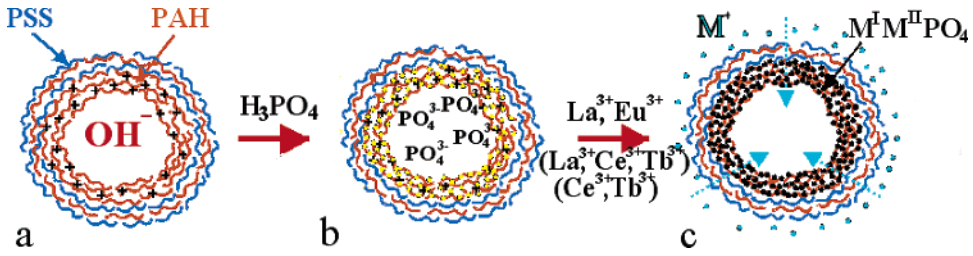

Figure 1. Schematic illustration of the synthesis of fluorescent rare earth phosphates inside polyelectrolyte capsules.

autoclaving). It seems possible to prepare fluorescent RE nanophosphates with perfect crystalline structure inside the capsule volume because of the slow and controlled diffusion of the reagents (multicharged ions) through polyelectrolyte multilayers and the strong influence of the confined reaction microvolume on the crystallization process.[32,33] Fluorescent RE nanophosphates can find application as label agents due to the fluorescent stability and smaller toxicity.[34] Q-dots such as CdS and CdSe, reported previously for biolabeling applications,[35,36] have two significant drawbacks: possible high toxicity[37,38] and low stability of the fluorescence in the presence of surfactants.

Experimental Section

Materials. Poly(allylamine hydrochloride) (PAH, MW ≈ 50 000), sodium poly(styrene sulfonate) (PSS, MW≈ 70 000), sodium citrate, NaCl, NaOH, H_3PO_4, $La(NO_4)_3{\cdot}6H_2O$, $Eu(NO_4)_3{\cdot}5H_2O$, $Tb(NO_4)_3{\cdot}5H_2O$, and $Ce(NO_4)_3{\cdot}6H_2O$ were obtained from Aldrich. All chemicals were used as received. The water used in all experiments was prepared in a three-stage Millipore Milli-Q Plus 185 purification system and had a resistivity higher than 18 MΩ·cm.

$MnCO_3$ template particles of 2.4 μm diameter for polyelectrolyte capsule assembly were synthesized by adding 0.5 mL of ethanol to 99.5 mL of 0.008 M $MnSO_4$ + 0.08 M NH_4HCO_3 solution at 50 °C.[39]

Fabrication of Initial Microcapsules. Hollow PAH/PSS capsules loaded with PAH were employed as microreactors for the synthesis of fluorescent RE nanophosphates. A mixture of $MnCO_3$ suspension (5×10^8 cm^{-3}) with a 5×10^{-3} M solution of citric acid was taken and then the PAH solution (1 mg/mL) was dropped with stirring. The deposition of the water-insoluble PAH/citrate complex on the surface of template particles was followed by layer-by-layer assembly of polyelectrolyte PAH/PSS multilayers with use of a 1 mg/mL of PAH solution and a 2 mg/mL of PSS solution in 0.5 M NaCl. After formation of PAH/PSS shells the $MnCO_3$ core was dissolved in 0.1 M HCl and hollow capsules composed of the inner thick PAH/citrate layer and outer PAH/PSS one were formed. A more detailed description of the synthesis of hollow PAH/PSS capsules can be found elsewhere.[9] Before loading the initial PAH/PSS capsules with PO_4^{3-} anions, the capsules were kept in NaOH solution, pH 9, for 24 h to replace citrate anions with OH^-.

Characterization. *Electron Microscopy.* Scanning electron microscopy (SEM) analysis was performed to investigate the outer structure and morphology of the synthesized polyelectrolyte shell/RE phosphate composite, using a Gemini Leo 1550 instrument operating at 3 keV. To view the interior of the capsules and to estimate the size of nanoparticles, the samples were embedded in poly(methyl methacrylate) and then ultrathin sections (30 to 100 nm in thickness) were obtained by a Leica ultracut UCT ultramicrotome. Carbon or noncoated copper grids were used to support the thin sections, and a Zeiss EM 912 Omega transmission electron microscope (TEM) was employed for analysis.

X-ray scattering. The crystallinity of the resulting nanosized rare earth phosphates was determined from wide-angle X-ray scattering, Enraf-Nonius PDS-120.

Quartz Crystal Microbalance Measurements. To measure the quantity of rare earth phosphates, we weighed an equal number of empty and loaded capsules with a quartz crystal microbalance (QCM). Equal quantities of empty and loaded capsules were estimated by taking into consideration different concentrations of the capsule suspension before and after phosphate synthesis measured by confocal fluorescence microscopy. QCM measurements were performed after drying the specimen in blowing air at 80 °C to evaporate water adsorbed in polyelectrolyte multilayers and the resulting nanomaterial.

Fluorescence Measurements. Confocal microscopy images of polyelectrolyte capsules in solution were obtained on a Leica TCS SP scanning system (Leica Microsystems Heidelberg) equipped with a 100× oil immersion objective and medium-pressure Hg lamp. The Hg lamp was placed perpendicular to the path of the scanning light to avoid the detection of its irradiation by microscope detectors. Only lines below 320 nm were used to excite rare earth phosphors. Lines of the Hg lamp at wavelengths more than 320 nm were cut off by a UV/vis filter setup. Images of the labeled polyelectrolyte capsules were taken by Leica Confocal Software version 2.5 (true-color fluorescence mode).

Fluorescence spectra of polyelectrolyte capsules filled with synthesized rare earth phosphates were recorded with a Spex Fluorolog 212 spectrofluorimeter (260 nm excitation line).

Elemental Analysis. Atomic analysis of the resulting rare earth nanophosphates was performed with a Perkin-Elmer Analyst 700 atomic absorbance spectrometer.

Results and Discussion

Three RE phosphates with different fluorescence spectra (red $La_{0.95}Eu_{0.05}PO_4$ and green $Ce_{0.9}Tb_{0.1}PO_4$ and $La_{0.4}Ce_{0.45}Tb_{0.15}PO_4$) were synthesized in the microvolume of polyelectrolyte capsules. These colors were chosen to develop a general approach for fabrication of rare earth nanophosphates in confined microvolume as well as to test these in situ synthesized nanoparticles as fluorescent labeling agents for polyelectrolyte capsules.

A standard synthetic protocol for the preparation of RE nanophosphates, which was reported in refs 24−26 and consists of the formation of mixed rare earth hydroxides on the first stage followed by transformation into phosphates by the reaction with $(NH_4)_2HPO_4$, was modified to correspond to the synthesis exclusively in the confined capsule microvolume. On the first stage, OH^- ions in the capsule volume were exchanged for PO_4^{3-} ions keeping the suspension of polyelectrolyte capsules in 0.25 M H_3PO_4 for 12 h (Figure 1a,b). These anions are enriched near the capsule wall in the form of a stable PAH/PO_4^{3-} complex.[40] Then, PO_4^{3-} loaded capsules were immersed into the solution of the corresponding rare earth salts (0.355 M $Ce(NO_4)_3{\cdot}6H_2O$ + 0.063 M $Tb(NO_4)_3{\cdot}5H_2O$ for $Ce_{0.9}Tb_{0.1}PO_4$;

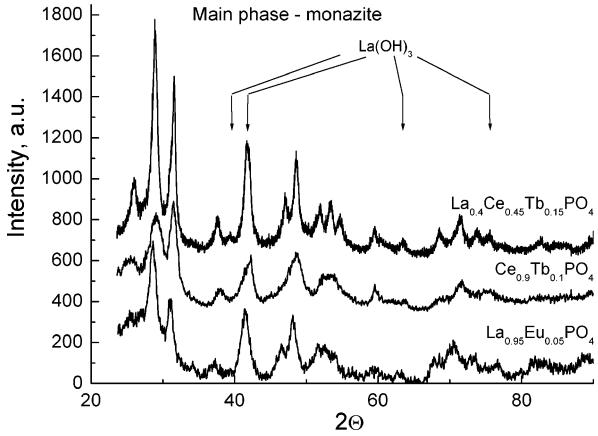

Figure 2. XRD patterns of nanocrystalline $La_{0.95}Eu_{0.05}PO_4$, $Ce_{0.9}Tb_{0.1}PO_4$, and $La_{0.4}Ce_{0.45}Tb_{0.15}PO_4$ synthesized inside polyelectrolyte capsules.

0.104 M $La(NO_4)_3 \cdot 6H_2O$ + 0.132 M $Ce(NO_4)_3 \cdot 6H_2O$ + 0.096 M $Tb(NO_4)_3 \cdot 5H_2O$ for $La_{0.4}Ce_{0.45}Tb_{0.15}PO_4$; 0.577 M $La(NO_4)_3 \cdot 6H_2O$ + 0.031 M $Eu(NO_4)_3 \cdot 5H_2O$ for red $La_{0.95}Eu_{0.05}PO_4$) for 7 days to complete crystallization of fluorescent phosphates inside polyelectrolyte capsules (Figure 1b,c). No changes in the mass of the nanophosphate-containing capsule were observed by QCM after 7 days of reaction while the mass of the capsule was gradually increasing within the first 7 days. Long reaction time, required for growth of inorganic nanoparticles inside polyelectrolyte capsules, was previously observed for hydroxyapatite synthesis.[41] This can be explained by a rather high stability of the PAH/phosphate complex, which maintains the concentration of PO_4^{3-} inside the capsules on a low but constant level making the gradual growth of phosphate nanoparticles possible. A similar effect is used in the so-called method of releasing reagent to form particles with good crystallinity from a solution of precursors complexed with strong ligands such as EDTA.[42] The average weight of RE nanodeposit is ca. 24 pg per capsule and does not depend on the material (as confirmed by QCM weighing of the samples) perhaps due to the same quantity of PO_4^{3-} ions in all initial, PO_4^{3-}-loaded capsules. It is important to emphasize that no additional heating is required to produce fluorescent rare earth phosphates inside the capsule microvolume while external autoclaving at 200 °C for 2 h is necessary to obtain these compounds in bulk solution.[24−26] The high crystallinity of the resulting $La_{0.95}Eu_{0.05}PO_4$, $Ce_{0.9}Tb_{0.1}PO_4$, and $La_{0.4}Ce_{0.45}Tb_{0.15}PO_4$ is confirmed by XRD analysis as shown in Figure 2. The X-ray diffraction patterns are similar for all three substances and are consistent with the monoclinic monazite structure known from bulk $LaPO_4$. The presence of the hydroxide phase in minor quantities was also indicated. As seen from XRD spectra of grown RE nanophosphates, no preferential orientation of nanorods during crystallization except the small deviation of the width of the peaks owing to the structure anisotropy is observed and their XRD patterns are similar to those of spherical RE nanophosphates described previously.[24]

Hence, it is possible to obtain crystalline nanocomposites inside polyelectrolyte capsules at ambient temperature (20 °C) because of the slow, gradual conditions of crystallization in the capsule volume. Possible changes of the solvent (water) structure inside micro- and submicrocapsules could also affect the crystallinity of the resulting nanocomposite. Atomic absorbance analysis of the nanophosphates formed inside the capsule volume confirmed (within experimental error) the theoretically predicted molar ratio of the components: $La_{0.946}Eu_{0.054}PO_4$ (known as $La_{0.95}Eu_{0.05}PO_4$), $Ce_{0.888}Tb_{0.112}PO_4$ (known as $Ce_{0.9}Tb_{0.1}PO_4$), and $La_{0.412}Ce_{0.439}Tb_{0.149}PO_4$ (known as $La_{0.4}Ce_{0.45}Tb_{0.15}PO_4$).

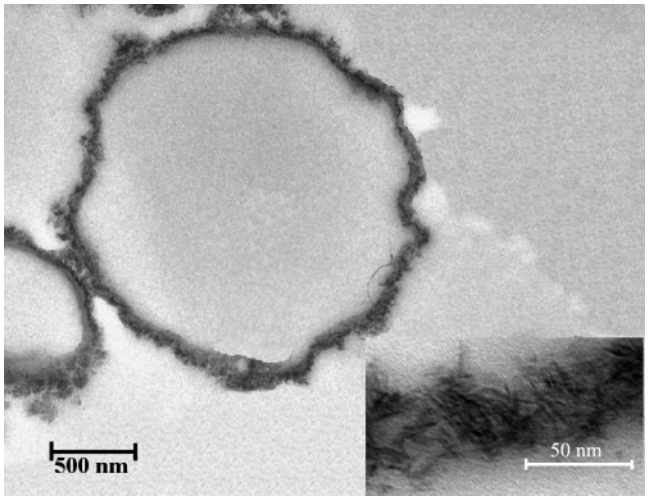

Figure 3. Transmission electron microscopy image of nano-$La_{0.95}Eu_{0.05}PO_4$ synthesized inside poly(allylamine hydrochloride)/poly(styrene sulfonate) polyelectrolyte capsules.

Figure 3 presents a transmission electron microscope image of ultramicrotomed polyelectrolyte capsules, containing synthesized $La_{0.95}Eu_{0.05}PO_4$ inside. In this image phosphate particles are seen as dark areas; the insert in Figure 3 shows RE phosphate at higher magnification. TEM analysis confirms the preferential formation of the RE phosphates presumably on the inner side of the PAH/PSS shell resulting in empty composite polyelectrolyte/RE phosphate spheres. Such a position of the reaction product can be due to the (i) higher concentration of the insoluble PAH/PO_4^{3-} complex and, as a consequence, PO_4^{3-} ions near the inner side of the capsule wall (as confirmed by confocal microscopy, results not shown), (ii) blocking of the shell pores by the resulting nanoparticles hindering, thereby, further diffusion of lanthanides to the capsule center. The $La_{0.95}Eu_{0.05}PO_4$ layer is ca. 70 nm thick and composed of crystalline rods f ca. 15 nm long and 4 nm in diameter. Other rare earth phosphates also formed similar hollow spheres. The formation of rodlike nanoparticles inside the thick inner shell of the polyelectrolyte capsule could be explained by the templating effect of polyelectrolyte multilayers. The crystallization process is governed by the pores of the polyelectrolyte multilayers, which results in various orientations of RE nanorods inside the polyelectrolyte shell and the absence of the preferable crystal alignment. A similar effect of meso- and nanoporous membranes acting as template media on the final morphology and crystallinity of inorganic nanomaterial was previously observed for silica and polymer membranes.[43,44]

Capsules containing synthesized RE nanophosphates are not spherical in the dried state, contrary to the capsules with hydroxyapatite nanoparticles in the shell,[41] and undergo partial collapse and shrinkage (∼10−15%, see comparison on SEM images in Figure 4a,b), however, they are mechanically more stable than the initial polyelectrolyte capsules without nanoparticle frame (Figure 3a),[45] which are flattered after drying. The outer morphology of the phosphate-loaded capsule shell is rough and reveals aggregates of nanoparticles formed in the capsule volume during drying.

To characterize the luminescence of RE phosphates, synthesized inside polyelectrolyte capsules, their emission spectra were recorded. Figure 5 shows the luminescence spectra of red $La_{0.95}Eu_{0.05}PO_4$ and two green $Ce_{0.9}Tb_{0.1}PO_4$ and $La_{0.4}Ce_{0.45}Tb_{0.15}PO_4$ types of particles formed inside the capsule volume. The

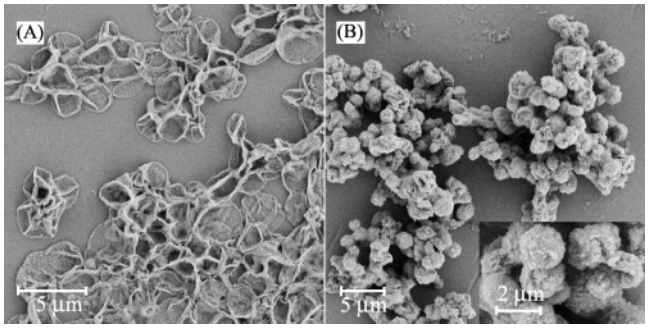

Figure 4. Scanning electron microscopy images of hollow polyelectrolyte capsules (a) and polyelectrolyte capsules with synthesized $La_{0.95}Eu_{0.05}PO_4$ inside (b).

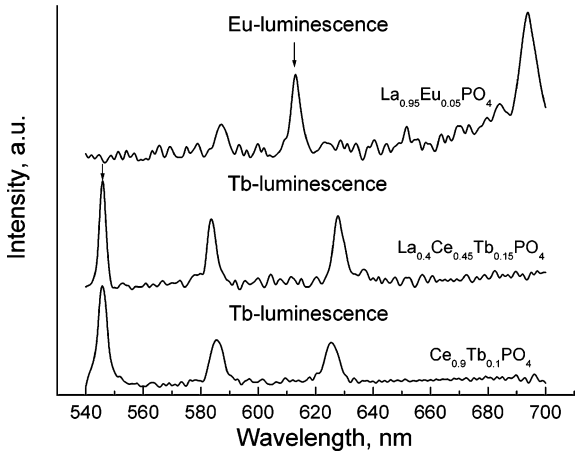

Figure 5. Luminescence spectra of $La_{0.95}Eu_{0.05}PO_4$, $Ce_{0.9}Tb_{0.1}PO_4$, and $La_{0.4}Ce_{0.45}Tb_{0.15}PO_4$ nanoparticles synthesized inside polyelectrolyte capsules ($\lambda_{ext} = 260$ nm).

luminescence spectra consisted of sharp lines for the transitions between europium (for $La_{0.95}Eu_{0.05}PO_4$, 588 and 614 nm) or terbium (for $Ce_{0.9}Tb_{0.1}PO_4$ and $La_{0.4}Ce_{0.45}Tb_{0.15}PO_4$, 545, 585, and 625 nm) d−f levels, which couple only very weakly to the lattice phonons.[30] For comparison, RE nanophosphates prepared in bulk solution at the same ambient conditions as for those synthesized inside polyelectrolyte capsules revealed extremely low fluorescence. Characteristic fluorescence peaks of the RE nanophosphates inside polyelectrolyte capsules appear at essentially the same spectral position as those for the corresponding nanoparticles prepared in bulk solution[26,30] after autoclaving at 200 °C.

Changing the pH of the capsule suspension does not result in complete disappearance of their luminescence properties (Figure 6). Reduction of the pH from neutral (pH 6.5) to acidic (pH 2) does not affect the intensity of the luminescence and peak position. Increasing the pH to 9 leads to partial quenching of the luminescence, which can be associated with hydrolysis of the lanthanide phosphates in alkaline media accompanied by formation of nonfluorescent hydroxides as confirmed by X-ray analysis.

The possibility of employing fluorescent rare earth phosphates of different color for labeling polyelectrolyte capsules was evaluated by using a medium-pressure Hg lamp for excitation and the confocal Leica TCS SP scanning system for registration of the fluorescence. A mixture of two sets of polyelectrolyte capsules containing red $La_{0.95}Eu_{0.05}PO_4$ or green $La_{0.4}Ce_{0.45}Tb_{0.15}PO_4$ inside is presented in the fluorescence mode in Figure 7. Two different types of capsules are clearly seen; however, the partial aggregation of the capsules is also observed at

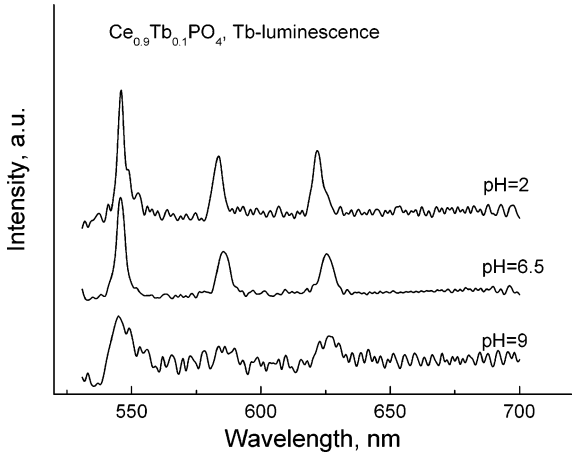

Figure 6. The influence of the pH value of the solution on the luminescence of $Ce_{0.9}Tb_{0.1}PO_4$ inside the capsule volume ($\lambda_{ext} = 260$ nm).

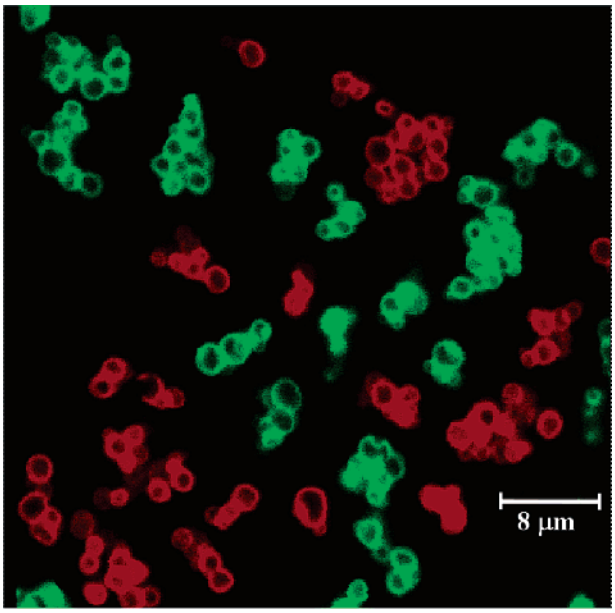

Figure 7. Fluorescence microscopy image of polyelectrolyte capsules labeled by two rare earth phosphates: (red) $La_{0.95}Eu_{0.05}PO_4$ and (green) $La_{0.4}Ce_{0.45}Tb_{0.15}PO_4$. Excitation was performed by a medium-pressure mercury lamp (wavelength range is <390 nm).

concentrations of the capsule suspension above 10^8 cm^{-3}. Reducing the concentration to 10^6 cm^{-3} leads to the decrease of the aggregated capsules resulting in 70% of individual capsules, the rest forming dimers and trimers. Rare earth phosphates, both individually and in combination to obtain superposition of their fluorescence, can be interesting alternatives for obtaining fluorescent polyelectrolyte capsules for further drug delivery and depot purposes.

Conclusions

We demonstrated that fluorescent rare earth nanophosphates (red $La_{0.95}Eu_{0.05}PO_4$ and green $Ce_{0.9}Tb_{0.1}PO_4$ and $La_{0.4}Ce_{0.45}Tb_{0.15}PO_4$) could be synthesized without additional thermal (autoclaving) treatment inside hollow polyelectrolyte capsules of 2.4 μm diameter. The resulting nanoparticles are crystalline rods ca. 15 nm long and 4 nm in diameter exhibiting fluorescence activity. They are gradually formed presumably near the inner side of the capsule shell. The synthetic approach developed

could be employed for the synthesis of other ordered inorganic nanocomposites inside the spatially confined microenvironment. The synthesized rare earth nanophosphates are stable at low and neutral pH, retaining their fluorescence properties. These nanoparticles can compete with quantum dots used previously for labeling polyelectrolyte capsules and other types of microcontainers.

Acknowledgment. This work was supported by the Sofja Kovalevskaja Program funded by the Alexander von Humboldt Foundation. D.S. acknowledges the Alexander von Humboldt Foundation for an individual research fellowship. The authors thank Dr. Jürgen Hartman, Rona Pitschke for ultramicrotoming and transmission electron microscopy analysis and Dr. Y. Wang for AAS measurements.

References and Notes

(1) Douglas, S. L.; Illum, L.; Davis, S. S.; Kreuter, J. *J. Colloid Interface Sci.* **1984**, *101*, 149.
(2) Lenaerts, V.; Couvreur, P.; Christiaensleyh, D. *Biomaterials* **1984**, *5*, 65.
(3) Debrander, M.; Geuens, G.; Nuydens, R. *Cytobios* **1985**, *43*, 273.
(4) Schmid, G., Ed. *Clusters and Colloids. From Theory to Applications*; Wiley-VCH: Weinheim, Germany, 1994.
(5) Fendler, J. H., Ed. *Nanoparticles and Nanostructured Films. Preparation, Characterization, and Application*; Wiley-VCH: Weinheim, Germany, 1998.
(6) Mamedov, A. A.; Belov, A.; Giersig, M.; Mamedova, N. N.; Kotov N. A. *J. Am. Chem. Soc.* **2001**, *123*, 7738.
(7) Yu, C.; Tian, B.; Fan, J.; Stucky, G. D.; Zhao, D. *Chem. Lett.* **2002**, *1*, 62.
(8) Ingert, D.; Pileni, M. P. *Adv. Funct. Mater.* **2001**, *11*, 136.
(9) Shchukin, D. G.; Sukhorukov, G. B. *Adv. Mater.* **2004**, *16*, 671.
(10) Li, M.; Mann, S. *Adv. Funct. Mater.* **2002**, *12*, 773.
(11) Pileni, M. P. *Catal. Today* **2000**, *58*, 151.
(12) Donath, E.; Sukhorukov, G. B.; Caruso, F.; Davis, S.; Möhwald, H. *Angew. Chem., Int. Ed.* **1998**, *37*, 2202.
(13) Decher, G.; Hong, J. D.; Schmitt, J. *Thin Solid Films* **1992**, *210*/*211*, 831.
(14) Dubas, S. T.; Schlenoff, J. B. *Macromolecules* **1999**, *32*, 8153.
(15) Ibarz, G.; Dahne, L.; Donath, E.; Möhwald, H. *Adv. Mater.* **2001**, *13*, 1324.
(16) Shchukin, D. G.; Radtchenko, I. L.; Sukhorukov, G. B. *J. Phys. Chem. B* **2003**, *107*, 952.
(17) Shchukin, D. G.; Radtchenko, I. L.; Sukhorukov, G. B. *ChemPhysChem* **2003**, *4*, 1101.
(18) Antipov, A.; Shchukin, D.; Fedutik, Y.; Zanaveskina, I.; Klechkovskaya, V.; Sukhorukov, G.; Möhwald, H. *Macromol. Rapid Commun.* **2003**, *24*, 274.
(19) Ghan, R.; Shutava, T.; Patel, A.; John, V.; Lvov Y. *Macromolecules* **2004**, *37*, 3615.
(20) Lee, I. S.; Hammond, P. T.; Rubner, M. F. *Chem. Mater.* **2003**, *15*, 4583.
(21) Bourcet, J. C.; Fong, F. K. *J. Chem. Phys.* **1974**, *60*, 34.
(22) Blasse, G.; Grabmaier. B. C., Eds. *Luminescent Materials*; Springer: Heidelberg, Germany, 1994.
(23) Kawano, K.; Arai, K.; Yamada, H.; Hashimoto, N.; Nakata, R. *Sol. Energy Mater. Sol. Cells* **1997**, *48*, 35.
(24) Meyssamy, H.; Riwotzki, K.; Kornowski, A.; Naused, S.; Haase, M. *Adv. Mater.* **1999**, *11*, 840.
(25) Riwotzki, K.; Meyssamy, H.; Schnablegger, H.; Kornowski, A.; Naused, S.; Haase, M. *Angew. Chem., Int. Ed.* **2001**, *40*, 573.
(26) Riwotzki, K.; Meyssamy, H.; Kornowski, A.; Haase, M. *J. Phys. Chem. B* **2000**, *104*, 2824.
(27) Erdei, S.; Ainger, F. W.; Ravichandran, D.; White, W. B.; Cross, L. E. *Mater. Lett.* **1997**, *30*, 389.
(28) Feldmann, C. *Adv. Funct. Mater.* **2003**, *13*, 101.
(29) Vanschaik, W.; Poort, S.; Blasse, G.; Omil, J.; Marquez S. *Chem. Mater.* **1994**, *6*, 755.
(30) Dexpert-Ghys, J.; Mauricot, R.; Faucher, M. D. *J. Lumin.* **1996**, *69*, 203.
(31) Cullell-Young, M.; Bayes, M.; Leeson, P. A. *Drug Future* **2003**, *28*, 224.
(32) Farhat, T. R.; Schlenoff, J. B. *Langmuir* **2001**, *17*, 1184.
(33) Harris, J. J.; Stair, J. L.; Bruening, M. L. *Chem. Mater.* **2000**, *12*, 1941.
(34) Schuetz, P.; Caruso, F. *Chem. Mater.* **2002**, *14*, 4509.
(35) Bruchez, M. P.; Moronne, M.; Gin, P.; Weiss, S.; Alivisatos, A. P. *Science* **1998**, *281*, 2013.
(36) Mamedova, N. N.; Kotov, N. A.; Rogach, A. L.; Studer, J. *Nano Lett.* **2001**, *1*, 281.
(37) Morgan, D. L.; Shines, C. J.; Jeter, S. P.; Blazka, M. E.; Elwell, M. R.; Wilson, R. E.; Ward, S. M.; Price, H. C.; Moskowitz, P. D. *Toxicol. Appl. Pharm.* **1997**, *147*, 399.
(38) Split decision on quantum dot toxicity. *Mater. Today* **2004**, *7*, no. 2.
(39) Hamada, S.; Kudo, Y.; Okada, J.; Kano, H. *J. Colloid Interface Sci.* **1987**, *118*, 356−365.
(40) Shchukin, D.; Sukhorukov, G. *Langmuir* **2003**, *19*, 4427.
(41) Shchukin, D. G.; Sukhorukov, G. B.; Möhwald, H. *Chem. Mater.* **2003**, *15*, 3947.
(42) Takahashi, M.; Muramatsu, Y.; Suzuki, T.; Sato, S.; Watanabe, M.; Wakita, K.; Uchida, T. *J. Electrochem. Soc.* **2003**, *150*, C169.
(43) Zhu, J.; Fan, S. *J. Mater. Res.* **1999**, *14*, 1175.
(44) Limmer, S. J.; Hubler, T. L.; Cao, G. *J. Sol.-Gel Sci. Technol.* **2003**, *26*, 577.
(45) Dubreuil, F.; Shchukin, D. G.; Sukhorukov, G. B.; Fery, A. *Macromol. Rapid Commun.* **2004**, *25*, 1078.